ELSEVIER

Journal of Photochemistry and Photobiology A: Chemistry 120 (1999) 191–199

Journal of Photochemistry and Photobiology A:Chemistry

# Photodynamic action of a water-soluble hypocrellin derivative with enhanced absorptivity in the phototherapeutic window II. Photosensitized generation of active oxygen species

Yu-Ying He, Jing-Yi An, Li-Jin Jiang*

*Institute of Photographic Chemistry, Academia Sinica, Beijing 100101, People's Republic of China*

Received 25 August 1998; received in revised form 16 October 1998; accepted 6 November 1998

**Abstract**

Cysteine-substituted hypocrellin B (Cys-HB) is a water-soluble perylenequinonoid derivative with significantly enhanced absorptivity in the range of wavelength longer than 600 nm. Electron paramagnetic resonance (EPR) measurements, quenching experiments and 9,10-diphenyl-anthracene bleaching studies were used to investigate the photodynamic action of Cys-HB in the presence of oxygen. Illumination of Cys-HB solution, in the presence of oxygen, generated singlet oxygen, superoxide anion radical, hydroxyl radical and hydrogen peroxide. The accumulation of active oxygen species was transformed into that of the semiquinone anion radical with the depletion of oxygen, detected by the spin counteraction of TEMPO radical formed via the reaction of TEMP with singlet oxygen produced by Cys-HB photosensitization. Oxygen content, Cys-HB concentration and reaction environment affected the transformation and the competition between the Type I and Type II reactions. Compared with hypocrellin B (HB), Cys-HB primarily remained similar and slightly lower capability of active oxygen-generation, confirmed to be a favorable phototherapeutic agent. 

*Keywords:* Cysteine-substituted hypocrellin B; Semiquinone anion radical; Active oxygen species; Electron paramagnetic resonance; Spin counteraction

## 1. Introduction

Hypocrellins, including hypocrellin A (HA) and hypocrellin B (HB), derive their names from *Hypocrella bambuase* (B. et Br), a parasitic fungus [1]. Their lipid-soluble perylenequinone derivatives were potent inhibitors of protein kinase C (PKC) [2], and could inactivate some types of viruses in the presence of visible light and oxygen [3–6]. These processes appeared to be mediated predominately by singlet oxygen ($^1O_2$). This was further supported by the extremely high quantum yield of $^1O_2$ generation by hypocrellins [7]. Also a variety of hypocrellin derivatives were demonstrated to be photodynamically active and efficient $^1O_2$ generators, including the sulfonated [8,9], aminated [10], halogenated [11] and metal ion-chelated compounds [11,12]. Zou and coworkers have reported the photodynamic action of HA in liposomes [13], and damage to pBR322 DNA derived from HA in liposomes and its derivative with the involvement of active oxygen species [14]. A series of comparative studies have indicated that 4,9-dihydroxy-3,10-perylenequinonoid moiety is the essential structural requirements for the generation of $^1O_2$ by hypocrellin-like compounds, while the side chains have minimal effect on the $^1O_2$ generating functions [7,15–17].

However, hypocrellins are insoluble in water and do not exhibit strong absorption in the domain of phototherapeutic windows. These disadvantages limited their application in clinical treatments. Therefore, HB was photochemically modified in the presence of cysteine to yield an aqueous soluble, far-red absorbing photosensitizer (Cys-HB) [18]. As a potential phototherapeutic agent, it is necessary to investigate the photodynamic action of Cys-HB, of which the photoinduced generation of the semiquinone anion radical and hydroquinone of Cys-HB in the absence of oxygen have been discussed in detail elsewhere [19]. Herein, we will report the photosensitized generation of active oxygen species in the presence of oxygen and the transformation between active oxygen mechanism to semiquinone anion radical; mechanism with the deplete of oxygen.

*Corresponding author. Tel.: +86-10-64888-068; fax: +86-10-620-29-375; e-mail: jyan@ipc.ac.cn

1010-6030/99/$ – see front matter 
PII: S1010-6030(98)00436-5

## 2. Materials and methods

### 2.1. Chemicals

HA was extracted from the fungus sacs of *Hypocrella bambusae* and recrystallization twice from acetone. HB was prepared by dehydration of HA [20]. 5,5-Dimethyl-1-pyrroline-N-oxide (DMPO) was purchased from Aldrich Chemical Company, and purified under argon and in the dark with activated charcoal prior to use. 2,2,6,6-tetramethyl-4-piperidone (TEMP), 2,2,6,6-tetramethyl-4-piperidone-N-oxyl radical (TEMPO), p-benzoquinone, 9,10-diphenyl-anthracene (DPA), sodium formate (HCOONa) and diethylene triamine pentaacetic acid (DTPA) were also obtained from Aldrich Chemical Company. 1,4-diazabicyclo[2,2,2]octane (DABCO) and dimethylsulfoxide (DMSO) were purchased from Merck Chemical Company. Catalase, superoxide dismutase (SOD), cysteine, reduced glutathione (GSH), reduced nicotinamide adenine dinucleotide (NADH) and histidine were obtained from Biotech Technology Corporation, Chinese Academy of Science (China). Mannitol, sodium benzoate, sodium azide ($NaN_3$), deuterated solvents and other agents of analytical grades were purchased from Beijing Chemical Plant (China).

pH of the irradiated solutions were adjusted, when necessary, by using the following buffer systems: citric acid–sodium hydroxide (for pH <6) and phosphate buffer (for pH 6–8.5).

Cys-HB was prepared according to He et al. [18] by photolysis of ethanol-buffer (1 : 3 by volume, pH >8) solution containing HB (0.1 mM) and cysteine (10 mM). A medium-pressure sodium lamp (450 W) was used as the light source, and 470 nm long-pass filters were used to cut off light of wavelength shorter than 470 nm. A water-jacketed cooling device was applied to maintain the temperature at 20°C. The reaction mixture was irradiated for 15 min, neutralized with 10% hydrochloric acid, extracted with chloroform and then evaporated under reduced pressure to afford bluish purple solid. The solid was subjected to 1% citric acid–silica gel thin-layer chromatography, using a 98 : 2 mixture of chloroform and methanol as developing agent and acetone as the eluent. Cys-HB was identified on the basis of UV–Vis, IR, $^1$H-NMR, MS data comparison with the published data [21].

### 2.2. Measurements of the water solubility of Cys-HB and HB

Partition coefficients of Cys-HB and HB between n-octanol and phosphate buffer (pH 7.4) were used to measure their water solubility. Cys-HB or HB (8 μM) was partitioned between n-octanol and 0.1 M phosphate buffer (pH 7.4). Both solvents were previously equilibrated with each other. After shaking for 2 min at 20°C, the phases were separated by centrifugation and the dye concentration was radiometrically measured in aliquots of both phases.

### 2.3. EPR measurements

Superoxide anion radical ($O_2^{\bullet -}$) and hydroxyl radical ($^{\bullet}OH$) were studied by means of spin trap of DMPO with EPR measurements. Singlet oxygen ($^1O_2$) was detected alternatively by EPR method with TEMP as spin trap [22] besides DPA-bleaching method (see below). The transformation of active oxygen species to the semiquinone anion radical of Cys-HB (Cys-$HB^{\bullet -}$) was investigated by spin counteraction of TEMPO from the reaction of $^1O_2$ and TEMP.

The EPR spectra were recorded at room temperature (22–24°C), using a Bruker ESP–300E spectrometer operating at 9.8 GHz equipped with a X-band of 100 kHz field modulation. A xenon arc lamp (1 kW) with an intensity of 23 W/m$^2$ was used as the light source equipped with a 540 nm long-pass filter. A water-jacketed cooling device was used to eliminate infrared emission. Samples were made in cuvettes, which allowed purging the reactive volume with argon, air or oxygen for 30 min in the dark, according to the experimental requirements, irradiated outside the cavity in the cuvettes, and then immediately transferred into quartz capillaries designed specially for EPR analysis after exposure.

### 2.4. Determination of the quantum yield of $^1O_2$ generation by DPA-bleaching method

The DPA-bleaching method was used to determine the $^1O_2$ generating quantum yields, the details of which were described in an earlier report [7]. The photo-oxidation of DPA sensitized by Cys-HB were carried out on a 'merry-go-round' apparatus, using a medium-pressure mercury lamp (500 W) as the light source. Filters were used in combination to isolate the 436 nm emission of the lamp (maximum transmittance, 45%). The reactions were followed spectrophotometrically by observing the decrease in the 374 nm-absorption peak of DPA (where the sensitizer used has the lowest absorptivity) as a function of irradiation time. In addition, the reaction of $^1O_2$ with TEMP in combination with EPR measurements was used to detect the formation of $^1O_2$ by Cys-HB in aqueous solution.

## 3. Results and discussion

The chromophore of Cys-HB is different from the perylenequinone structure of HB (Fig. 1) owing to the nitrogen atom substitution for oxygen atom at the carbonyl group. The water solubility of Cys-HB (7.2) was significantly improved compared with that of HB (46.4) in terms of their partition coefficients between n-octanol and phosphate buffer (pH 7.4). The absorption peak shifted red to 710 nm (log $\varepsilon = 4.06$) where HB had little absorption (Fig. 2). All of these aspects motivate the investigations on the photodynamic action of Cys-HB. The type I mechanism of Cys-HB

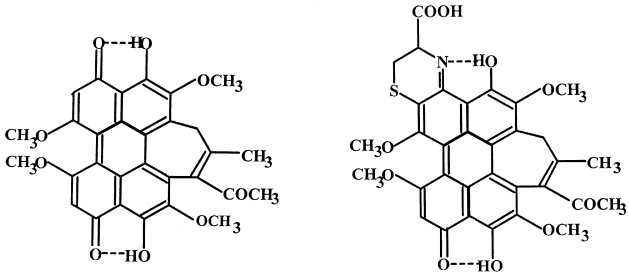


Fig. 1. Chemical structures of HB (left) and Cys-HB (right).

in the absence of oxygen has been discussed elsewhere in detail [19]. Herein, we will survey the generation of active oxygen species in the presence of oxygen by Cys-HB photosensitization.

### 3.1. Generation of superoxide anion radical ($O_2^{\bullet -}$)

Irradiation of Cys-HB (1 mM) DMSO solution in the absence of oxygen generated an EPR spectrum ascribed to the semiquinone anion radical of Cys-HB (Cys-HB$^{\bullet -}$), which has been discussed elsewhere in detail [19]. The photoinduced EPR spectrum of Cys-HB$^{\bullet -}$ disappeared when oxygen was bubbled through the argon-saturated DMSO-buffer (1 : 1 by volume, pH 8.0) containing Cys-HB (1 mM) and NADH (5 mM) after illumination [19]. When oxygen and DMPO were involved in the reaction system, the EPR signal of DMPO-superoxide radical adduct was observed [19]. This suggested the oxidation of Cys-HB by dissolved oxygen and the formation of superoxide anion radical ($O_2^{\bullet -}$). Subsequent experiments were carried out in order to examine this process and the $O_2^{\bullet -}$ generating capacity of Cys-HB. It is known that $O_2^{\bullet -}$ is relatively stable in aprotic solvents, where no free hydrogen ions ($H^+$), necessary for the dismutation of $O_2^{\bullet -}$, are accessible. For this reason, the experiments were performed in DMSO.

When an aerated DMSO solution containing Cys-HB (0.1 mM) and DMPO (50 mM) was irradiated, an EPR spectrum appeared immediately (Fig. 3(B)). The EPR spectrum was characterized by three coupling constants, which are due to the nitrogen atom and two hydrogen atoms at the $\beta$ and $\gamma$ positions. The $g$ factor and the determined constants ($g = 2.0056$, $a^N = 13.0$ G, $a_\beta^H = 10.0$ G and $a_\gamma^H = 1.4$ G) are in good agreement with the literature for DMPO-superoxide radical adduct [23]. Control experiments (Fig. 3(A)) confirmed that Cys-HB, oxygen and irradiation were all necessary to produce the EPR signal shown in Fig. 3(B). The addition of SOD (40 μg/ml) prior to illumination inhibited the EPR signal significantly (Fig. 3(D)). The presence of the thermally denatured SOD did not affect the signal. The EPR signal was also suppressed by p-benzoquinone (4 mM), an efficient scavenger of $O_2^{\bullet -}$ [24]. These observations confirmed the correct assignment of the EPR spectrum to DMPO-$O_2^{\bullet -}$ adduct.

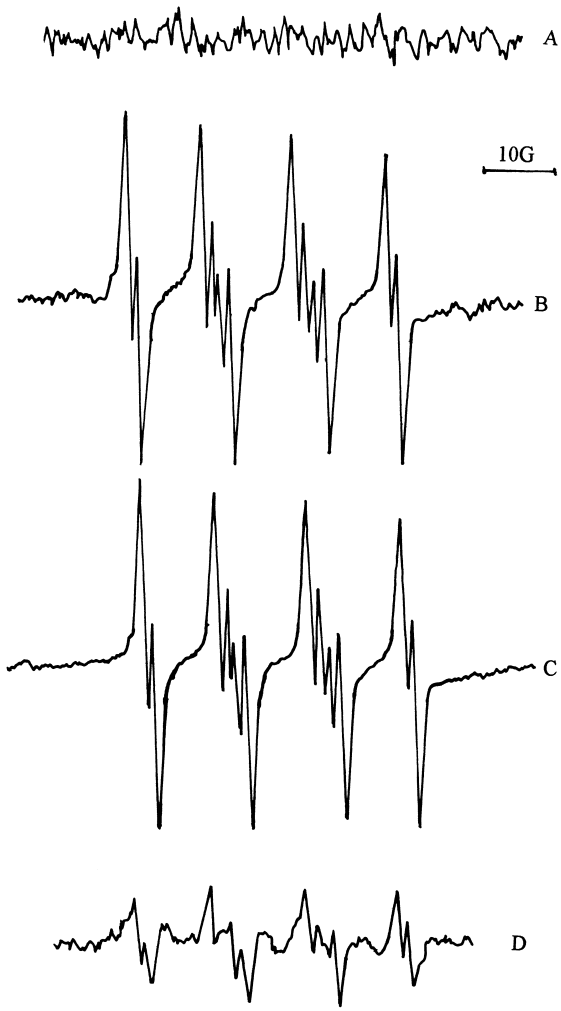


Fig. 3. EPR spectra of DMSO-superoxide radical adduct produced from irradiation of an oxygen-saturated DMSO solution of Cys-HB (0.1 mM) and DMPO (50 mM). (A) Removal of Cys-HB, oxygen or light, (B) On irradiation for 2 min, receiver gain: $5 \times 10^4$, (C) As in (B) but in the presence of NADH (5 mM), receiver gain: $5 \times 10^3$, (D) As in (B) but in the presence of SOD (40 μg/ml), receiver gain: $5 \times 10^4$. (Instrumental settings: microwave power, 8 mW; modulation amplitude, 1 G; scan range, 200 G).

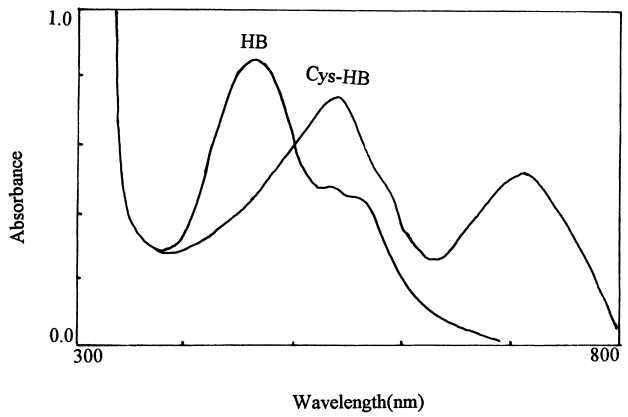


Fig. 2. Absorption spectra of HB and Cys-HB in chloroform.

The addition of NADH, a typical electron donor, significantly enhanced the EPR signal intensity of DMPO-$O_2^{\bullet -}$ adduct (Fig. 3(C)). It was found that the addition of NADH (5 mM) resulted in a nearly tenfold enhancement in $O_2^{\bullet -}$ production. In addition, the presence of other electron donors, such as cysteine, mercaptoethanol, reduced glutathione and ascorbic acid also significantly enhanced the EPR signal of the DMPO-$O_2^{\bullet -}$ adduct. Similarly, the addition of electron donors could promote the formation of the semiquinone anion radical of Cys-HB (Cys-$HB^{\bullet -}$) [19]. The consistent effect of electron donors on the formation of $O_2^{\bullet -}$ and that of Cys-$HB^{\bullet -}$ suggested that Cys-$HB^{\bullet -}$ was the precursor for the generation of $O_2^{\bullet -}$ by Cys-HB photosensitization. In the absence or presence of electron donors, Cys-$HB^{\bullet -}$ could be formed via the reaction shown in Eq. (1) or Eq. (2) and then transfers one electron to oxygen to form $O_2^{\bullet -}$ via Eq. (3) in the presence of oxygen.

$$\text{Cys-HB}^* + \text{Cys-HB} \rightarrow \text{Cys-HB}^{\bullet -} + \text{Cys-HB}^{\bullet +} \quad (1)$$

$$\text{Cys-HB}^* + \text{D} \rightarrow \text{Cys-HB}^{\bullet -} + \text{D}^{\bullet +} \quad (2)$$

$$\text{Cys-HB}^{\bullet -} + \text{O}_2 \rightarrow \text{Cys-HB} + \text{O}_2^{\bullet -} \quad (3)$$

Attempts were also made to compare the efficiency of $O_2^{\bullet -}$ generation by Cys-HB with that of HB. Fig. 4 suggested that Cys-HB (Fig. 4(A)) could photosensitize the generation of $O_2^{\bullet -}$ with lowered efficiency compared with HB (Fig. 4(B)). In addition, a decrease of Cys-HB concentration reduced the $O_2^{\bullet -}$ generation significantly (Fig. 4(C)). The $O_2^{\bullet -}$ production was also dependent on the dissolved oxygen content. The EPR signal intensity obtained from aerated sample was less than that from oxygen-saturated sample (Fig. 4(D)) and no DMPO-$O_2^{\bullet -}$ signal was detected in the absence of oxygen. The EPR signal of DMPO-$O_2^{\bullet -}$ was scarcely detected in aqueous buffer solution (pH 7.4) (Fig. 4(E)) or acidic DMSO-buffer (1 : 1 by volume, pH 5.6) solution (Fig. 4(F)). In the absence of catalase, an EPR signal of DMPO-hydroxyl radical adduct was observed (see below), since the ratio of the reacting rate constants of DMPO with hydroxyl to that of superoxide radical is of in the order of $10^5$. It is evident that the reaction of DMPO with a hydroxyl radical will significantly prevail over that with a superoxide radical even when the superoxide radical is the precursor and its concentration is much higher. This was also consistent with the generation of Cys-$HB^{\bullet -}$ [19] which was not detected by EPR but was confirmed by spin counteraction of TEMPO in aqueous solution or in DMSO-buffer (1 : 1 by volume, pH 5.6). The latter was owing to the shortened lifetime of Cys-$HB^{\bullet -}$ by the acceleration of the disproportionation of and second electron transfer to Cys-$HB^{\bullet -}$ to form hydroquinone in the presence of electron donors. The reaction of hydroquinone formation competed with that of $O_2^{\bullet -}$ generation shown in Eq. (3), which would reduce the generation of $O_2^{\bullet -}$ concomitantly.

### 3.2. Transformation of $O_2^{\bullet -}$ into $^{\bullet}OH$

A weak EPR spectrum of the spin adduct of DMPO-$^{\bullet}$OH (Fig. 5(A)) was observed when DMPO (50 mM) was added into an oxygen-saturated aqueous solution of Cys-HB (0.1 mM, pH 7.4). This background arose owing to the preparation of samples in scattered daylight and disappeared if samples were prepared and analyzed in the dark (Fig. 5(B)). After illumination of the sample with visible light of wavelength longer than 540 nm, the intensity of the DMPO-$^{\bullet}$OH spectrum (Fig. 5(C)) increased by 15 times as much as that of unirradiated sample shown in Fig. 5(A). The quartet with an intensity ratio of 1 : 2 : 2 : 1 and character-

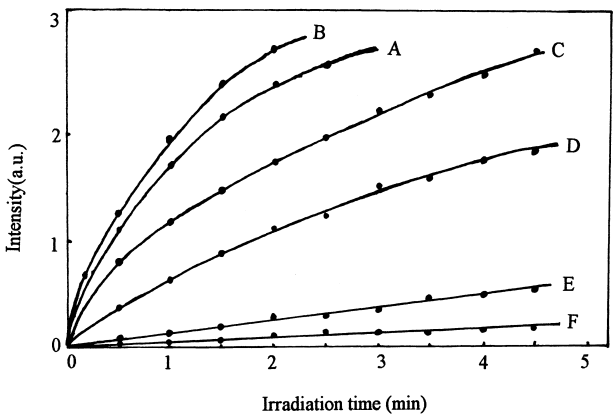


Fig. 4. Signal intensity of the spin-adduct DMPO-superoxide during illumination of solution of Cys-HB or HB and DMPO (50 mM) (a.u. – arbitrary unit). (A) Oxygen-saturated DMSO solution of Cys-HB (0.1 mM), (B) Oxygen-saturated DMSO solution of HB (0.1 mM), (C) Oxygen-saturated DMSO solution of Cys-HB (50 μM), (D) Aerated DMSO solution of Cys-HB (0.1 mM), (E) Oxygen-saturated buffer solution (pH 7.4) of Cys-HB (0.1 mM) and DMPO (0.5 M) in the presence of catalase, (F) Same as (E) but instead in DMSO-buffer (1 : 1 by volume, pH 5.6) solution and DMPO (0.5 M) in the presence of catalase.

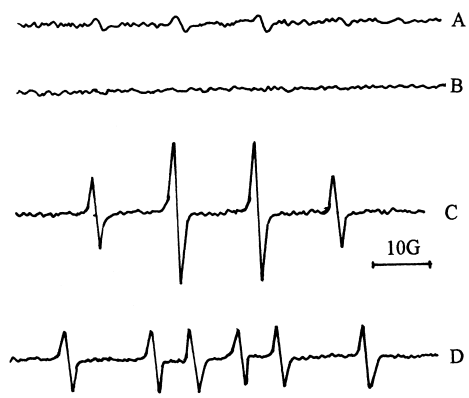


Fig. 5. EPR spectra of DMPO-hydroxyl radical adduct produced from irradiation of an oxygen-saturated buffer solution of Cys-HB (0.1 mM, pH 7.4) and DMPO (50 mM). (A) sample prepared in the daylight, (B) In the absence of Cys-HB or oxygen or irradiation. (C) On irradiation for 2 min, (D) As in (C) but in the presence of $CH_3CH_2OH$ and the solution was incubated in the dark for 2 min after irradiation. (Instrumental settings – microwave power, 8 mW; modulation amplitude, 1 G; scan range, 200 G; receiver gain, $1 \times 10^4$).

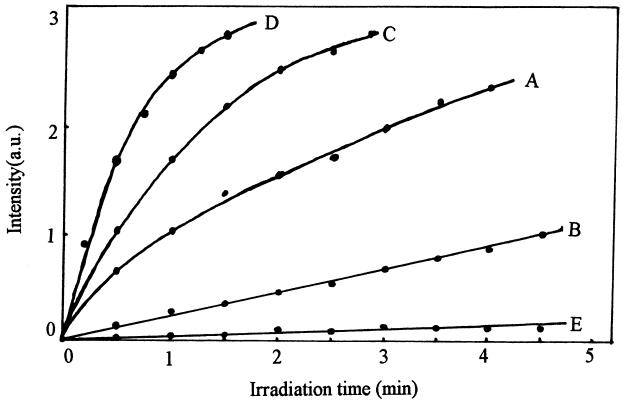


Fig. 6. Dependence of the EPR signal intensity (a.u. – arbitrary unit) on the irradiation time formed from irradiation of the aqueous solutions of Cys-HB and DMPO (50 mM). (A) Oxygen-saturated Cys-HB (0.1 mM) solution, (B) Aerated Cys-HB (0.1 mM) solution, (C) Oxygen-saturated Cys-HB (0.2 mM) solution, (D) As in (A) but in the presence of NADH (5 mM). (E) As in (A) but in the presence of catalase (30 μg/ml).

istic constants ($g = 2.0054$, $a^N = a^H = 14.9$ G) were in good agreement with those found in the literature [22]. When ethanol (0.1 M) was introduced into the sample, the EPR spectrum of DMPO-$CH_3^{\bullet}CHOH$ adduct with $a^N = 16.0$ G and $a^H = 23.5$ G was observed (Fig. 5(D)). When DMSO (20 mM), acting as a scavenger of hydroxyl radical was added to the sample, the quartet disappeared and EPR signal of DMPO-$^{\bullet}CH_3$ ($a^N = 16.0$ G, $a^H = 23.0$ G, similar to those of EPR signal of DMPO-$CH_3^{\bullet}CHOH$ shown in Fig. 5(D)) appeared (not shown). The presence of other $^{\bullet}OH$ quenchers such as mannitol and sodium benzoate showed similar results to DMSO. These observations confirmed the correct assignment of the spectrum shown in Fig. 5(C) to the DMPO-$^{\bullet}OH$ radical adduct. In addition, the production of $^{\bullet}OH$ by Cys-HB depended on the concentration of Cys-HB, oxygen, irradiation intensity and time. No EPR signal of DMPO-$^{\bullet}OH$ adduct was detected in the absence of Cys-HB, oxygen or irradiation (Fig. 5(B)). The intensity of DMPO-$^{\bullet}OH$ signal increased with the irradiation time (Fig. 6). The EPR signal intensity of DMPO-$^{\bullet}OH$ increased with an increase of Cys-HB concentration (Fig. 6C) and decreased with the replacement of oxygen by air (Fig. 6(B)). The presence of electron donors significantly enhanced the production of hydroxyl radical (Fig. 6(D)). The addition of catalase (30 μg/ml) significantly reduced the EPR signal intensity of DMPO-$^{\bullet}OH$. The latter suggested that $^{\bullet}OH$ generation by Cys-HB photosensitization was $H_2O_2$ dependent.

The addition of ferric EDTA enhanced the EPR signal of the DMPO-$^{\bullet}OH$ adduct (Fig. 7(B)). Therefore, the formation of hydroxyl radicals was inferred via the participation of Haber-Weiss reaction or superoxide-driven Fenton reaction by Cys-HB photosensitization (Eqs. (4) and (5)), where $H_2O_2$ originated from the dismutation

$$Fe^{3+} + O_2^{\bullet -} \rightarrow Fe^{2+} + O_2 \quad (4)$$

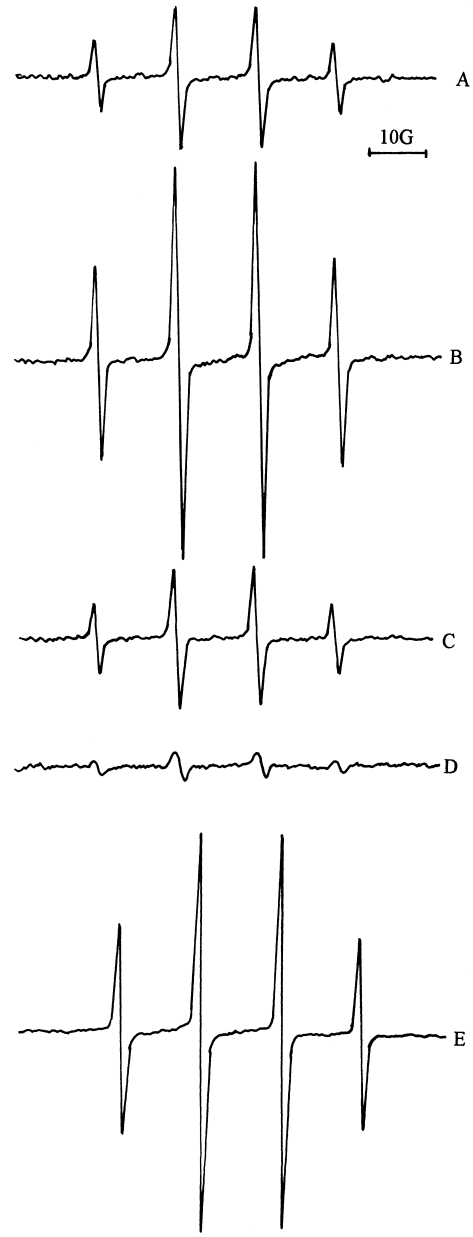


Fig. 7. (A) EPR spectra of DMPO-hydroxyl radical adduct produced from irradiation of an oxygen-saturated buffer solution of Cys-HB (0.1 mM, pH 7.4) and DMPO (50 mM), (B) As in (A) but in the presence of ferric EDTA (50 μM), (C) As in (A) but in the presence of SOD (25 μg/ml), (D) As in (A) but in the presence of DTPA (5 mM), (E) EPR spectrum of DMPO-hydroxyl radical adduct produced from irradiation of an argon-saturated aqueous solution containing Cys-HB (0.1 mM), $H_2O_2$ (0.1 mM), DTPA (5 mM) and DMPO (50 mM). (Instrumental settings – microwave power, 8 mW; modulation amplitude, 1 G; scan range, 200 G; receiver gain, $1 \times 10^4$ for A, B, C, D and $1 \times 10^3$ for E).

$$Fe^{2+} + H_2O_2 \rightarrow Fe^{3+} + {}^{-}OH + HO^{\bullet} \quad (5)$$

of superoxide radical ($O_2^{\bullet -}$) (Eq. (6)). Iron ions acted as the catalyst in the formation of hydroxyl radical. However, the following reactions might also take place in the system to participate in the $^{\bullet}OH$ generation due to the reductivity of Cys-HB$^{\bullet -}$ like ferrous ion (Eq. (7) and Eq. (8)). These

expectations were confirmed by the following experiments.

$$O_2^{\bullet -} + O_2^{\bullet -} \xrightarrow{H^+ \text{or SOD}} H_2O_2 + O_2 \quad (6)$$

$$Fe^{3+} + \text{Cys-HB}^{\bullet -} \rightarrow Fe^{2+} + \text{Cys-HB} \quad (7)$$

$$H_2O_2 + \text{Cys-HB}^{\bullet -} \rightarrow {}^{\bullet}OH + {}^{-}OH + \text{Cys-HB} \quad (8)$$

1. The addition of SOD (25 μg/ml) to the irradiated solution of Cys-HB showed no obvious effect on the EPR signal of DMPO-hydroxyl radical adduct (Fig. 7(C)). This is because that the dismutation of $O_2^{\bullet -}$ catalyzed by SOD also produced $H_2O_2$ (Eq. (6)), and the formation of $HO^{\bullet}$ was $H_2O_2$ dependent. This confirmed that the reaction in Eq. (7) took place in the system coexistently with that in Eq. (4).
2. The addition of DTPA up to 8 mM could not eliminate the EPR signal of DMPO-$^{\bullet}$OH adduct completely (Fig. 7(D)), confirming the participation of the reaction shown in Eq. (8).
3. Irradiation of an argon-saturated aqueous solution containing Cys-HB (0.1 mM), $H_2O_2$ (0.1 mM), DTPA (5 mM) and DMPO (50 mM) with light of wavelength longer than 540 nm generated a strong EPR signal of DMPO-$^{\bullet}$OH adduct (Fig. 7(E)).

These experiments strongly supported that the pathways shown in Eq. (7) and Eq. (8) were involved in the formation of hydroxyl radical in the photosensitizing system.

### 3.3. Generation of singlet oxygen ($^1O_2$) by Cys-HB

The photooxidation of DPA to its endoperoxide derivative by singlet oxygen Eq. (9) is usually used to detect singlet oxygen formed from photosensitization [7]. In order to determine the quantum yield of $^1O_2$ generation by Cys-HB photosensitization, the DPA-bleaching method was adopted and HB was used as the reference ($\phi_{^1O_2} = 0.76$) [7]. During the measurements, the concentration of Cys-HB remained constant at 76 μM and the absorption of HB at 436 nm used was adjusted to be the same as those of Cys-HB solution (0.7 in a 10 mm × 10 mm cell).

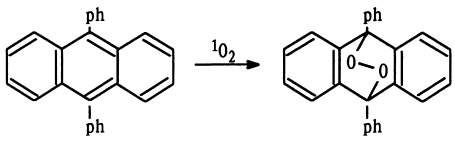


(9)

$$\text{Cys-HB} \xrightarrow{h\nu} {}^1\text{Cys-HB} \xrightarrow{\text{isc}} {}^3\text{Cys-HB} \xrightarrow{O_2} \text{Cys-HB} + {}^1O_2 \quad (10)$$

The rates of DPA bleaching photosensitized by Cys-HB in $CHCl_3$ (Line 1), HB in $CHCl_3$ (Line 2) and Cys-HB in $CDCl_3$ (Line 3) and the control (Line 4) are demonstrated in Fig. 8. It is obvious from Line 4 that no DPA was bleached in the absence of Cys-HB, oxygen or irradiation. The DPA bleaching rate of Cys-HB in $CDCl_3$ (Line 3) increased

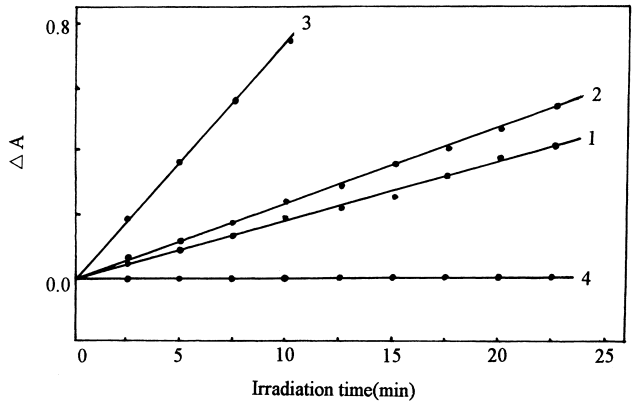


Fig. 8. Photosensitized DPA-bleaching measured via the absorbance decreases (ΔA) of DPA at 374 nm as a function of irradiation time in minutes: Line 1, Cys-HB in $O_2$-saturated $CHCl_3$; Line 2, HB in $O_2$-saturated $CHCl_3$; Line 3, Cys-HB in $O_2$-saturated $CDCl_3$; Line 4, in the absence of Cys-HB, oxygen or irradiation.

nearly by four times as much as that in $CHCl_3$ (Line 1) because the lifetime of $^1O_2$ in deuterated solvents increased by ten to fifteen times as long as that in non-deuterated solvents. These results showed that singlet oxygen was produced from Cys-HB photosensitization with the participation of oxygen Eq. (10) and that DPA was then bleached via the reaction shown in Eq. (9). Further support for this was provided by DABCO inhibiting experiments. Fig. 9 shows the Stern–Volmer plot for the effect of DABCO, a typical $^1O_2$ inhibitor, on the bleaching of DPA by Cys-HB photosensitization. As was shown in this figure, the Stern-Volmer behavior for DABCO quenching remained linear up to at least 1 mM DABCO. The bimolecular quenching rate constant for DABCO was estimated according to dynamic quenching [25]

$$\phi = \frac{K_T[\text{DPA}]}{K_q[\text{Q}] + K_T[\text{DPA}] + K_d}$$

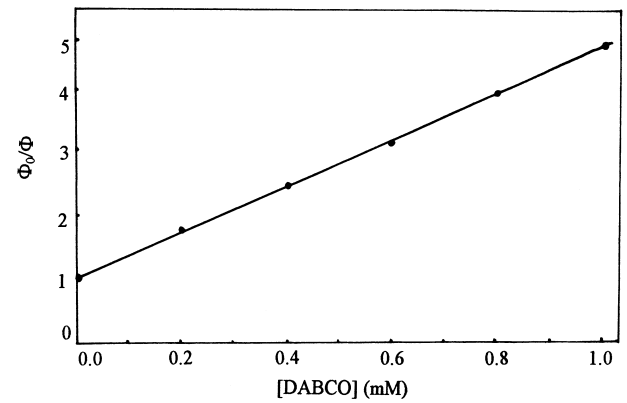


Fig. 9. Stern–Volmer plot of DABCO quenching on DPA-bleaching during Cys-HB photosensitization, performed by adding various amounts of DABCO to a series of $O_2$-saturated $CHCl_3$ solution containing Cys-HB (76 μM) and DPA (0.54 mM).

where $\phi$ is the quantum yield of DPA photobleaching, $K_T$ is the rate constant for DPA ($1.3 \times 10^6\ M^{-1}\ s^{-1}$ [26]), $K_d$ is the decay rate constant of $^1O_2$ in $CHCl_3$ ($\tau = 160\ \mu s$ [27]), and $K_q$ and [Q] are the rate constant and concentration for DABCO. From this, it follows that

$$\frac{\phi_0}{\phi} = 1 + \frac{K_q}{K_T[DPA] + K_d}[Q]$$

The estimated rate constant for DABCO quenching was $2.4 \times 10^7\ M^{-1}\ s^{-1}$ in $CHCl_3$, which is in reasonable agreement with that obtained by Monroe [28] for the reaction of DABCO with $^1O_2$ ($2 \times 10^7\ M^{-1}\ s^{-1}$), suggesting that Cys-HB does indeed generate singlet oxygen upon irradiation. Fig. 8 shows that HB can also efficiently photosensitize the generation of $^1O_2$ and it is about 1.27 times as effective as Cys-HB. The quantum yield of $^1O_2$ generation for Cys-HB in $CHCl_3$ is thus estimated to be 0.60 using $\phi_{^1O_2} = 0.76$ for HB.

In addition, the $^1O_2$ generation photosensitized by Cys-HB in DMSO and aqueous solution was investigated by EPR measurements, using TEMP as a spin trap. Moan and Wold [22] have reported that TEMP can easily react with $^1O_2$ to yield a nitroxide, i.e. TEMPO via Eq. (11) which can be detected by EPR spectroscopy. Irradiation of

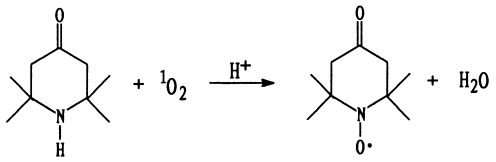


(11)

oxygen-saturated solutions containing Cys-HB (0.1 mM), SOD (40 μg/ml), HCOONa (0.1 M) and TEMP (20 mM) afforded typical three-line EPR spectra with $a^N = 16.0$ G and $g = 2.0056$ in DMSO (Fig. 10(A)), buffer (pH 7.4) (Fig. 10(B)) and in $CHCl_3$ with TEMP (20 mM) (Fig. 10(C)), respectively, which were in agreement with the literature [22] and ascribed to that of TEMPO. The addition of $NaN_3$ or histidine inhibited the EPR signals shown in Fig. 10(A)–(B) significantly (Fig. 10(D)–(E)). These observations confirmed that the TEMPO signal came from the reaction of TEMP with $^1O_2$ during Cys-HB photosensitization. It can also be seen from Fig. 10 that the intensity of TEMPO signal in water decreased by about 20 times compared with that in $CHCl_3$ and in DMSO. The quantum yield of TEMPO formation ($\phi_T$) follows that

$$\phi_T = \frac{K_T[TEMP]}{K_T[TEMP] + K_d}$$

where $\phi_T$ and $K_T$ are the quantum yield and rate constant of TEMPO formation respectively, $K_T = 2 \times 10^5\ M^{-1}\ s^{-1}$ determined by Lion et al. [30], $K_d$ is the decay rate constant of $^1O_2$ ($\tau = 160\ \mu s$ in $CHCl_3$ [27] and $\tau = 7\ \mu s$ in water [29]). From this, the ratio of $\phi_T$ in $CHCl_3$ to that in water was estimated to be approximately 14. Thus, the greatly shortened lifetime of $^1O_2$ in water was predominantly responsible for the significant decrease of $\phi_T$.

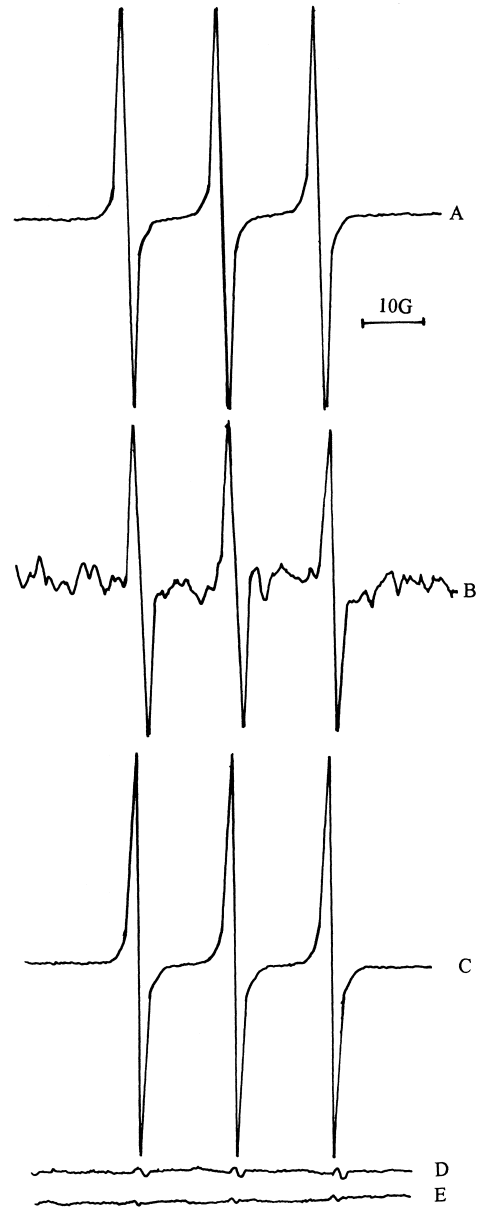


Fig. 10. EPR spectra obtained from irradiation of an oxygen-saturated solution of Cys-HB (0.1 mM), SOD (40 μg/ml), HCOONa (0.1 M) and TEMP (20 mM). (A) In DMSO, gain $1 \times 10^4$, (B) In buffer (pH 7.4) solution, gain $2 \times 10^5$, (C) In $CHCl_3$, gain $1 \times 10^4$, (D) As in (A) but in the presence of histidine (1 mM), (E) As in (B) but in the presence of $NaN_3$ (1 mM). (Instrumental settings – microwave power, 8 mW; modulation amplitude, 1 G; scan range, 200 G).

### 3.4. Transformation between active oxygen species and the semiquinone anion radical of Cys-HB

It has been investigated in detail (see above) that active oxygen species ($^1O_2$, $^\bullet OH$ and $O_2^{\bullet -}$) can be generated by Cys-HB photosensitization in the presence of oxygen. However, only the semiquinone anion radical of Cys-HB (Cys-$HB^{\bullet -}$) rather than active oxygen species is formed during irradiation in the absence of oxygen. It is obvious that oxygen plays an important role in the determination of

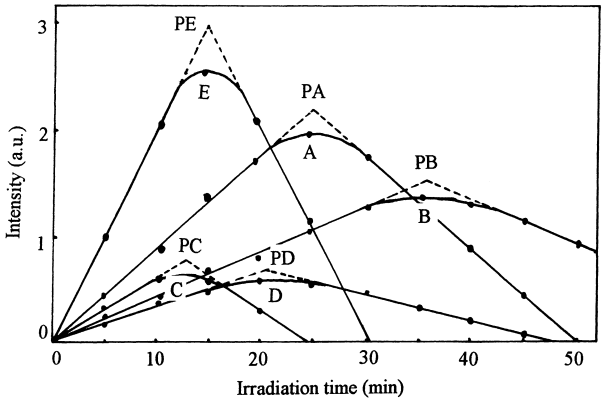


Fig. 11. Dependence of the intensity of TEMPO signal on the irradiation time when the sealed system Cys-HB (1 mM) and TEMPO (20 mM) was irradiated. (A) From the oxygen-saturated DMSO solution, (B) From the oxygen-saturated DMSO-buffer (1 : 1 by volume, pH 8.0) solution, (C) From the aerated DMSO solution, (D) From the oxygen-saturated DMSO solution of Cys-HB (0.1 mM), (E) From the oxygen-saturated DMSO solution of HB (0.1 mM). (Instrumental settings – microwave power, 8 mW; modulation amplitude, 1 G; scan range, 200 G; receiver gain, $1 \times 10^5$).

PDT mechanism. The unique and dual role of TEMPO, formed during $^1O_2$ generation, and capable of detecting Cys-HB$^{\bullet -}$ [19], can be conveniently taken advantage of for detecting the transformation between $^1O_2$ and Cys-HB$^{\bullet -}$ as oxygen concentration changes. When the sealed DMSO solution of oxygen-saturated Cys-HB (1 mM) and TEMP (20 mM) was irradiated, the EPR signal intensity of TEMPO increased to the maximum within about 25 min and then decreased as irradiation proceeded (Fig. 11(A)). The increasing process of TEMPO signal intensity was caused by the reaction of TEMP with $^1O_2$ shown in Eq. (11), and the eliminating process of TEMPO resulted from the reaction of Cys-HB$^{\bullet -}$ with TEMPO by Cys-HB photosensitization in hypoxic solution [19] shown in Eq. (12). The decrease of oxygen concentration in the sealed solution caused by the reaction shown in Eq. (8) suppressed the formation of $^1O_2$ but promoted the production of Cys-HB$^{\bullet -}$. The turning point (PA) in Fig. 11(A) indicated that the accumulation of $^1O_2$ was replaced by that of Cys-HB$^{\bullet -}$ and that oxygen was exhausted. This showed that oxygen played a critical role in the competition and transformation between Type I and Type II mechanisms of Cys-HB photosensitization.

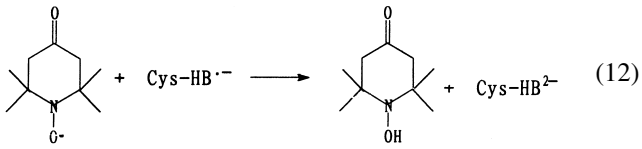


(12)

In addition, the effects of oxygen content, Cys-HB concentration and water content in the sealed system were surveyed. The increase of water content delayed the appearance of the turning point (PB, in Fig. 11(B)) with the reduced maximum. This was consistent with the decrease of $^1O_2$ production in aqueous solution (see above). When an aerated sample instead of oxygen-saturated sample was irradiated, the turning point (PC, in Fig. 11(C)) appeared earlier concomitantly with a decrease in the maximum. And the decrease of Cys-HB concentration rendered the earlier appearance of turning point (PD, in Fig. 11(D)) and with the decreased maximum. The comparison of the transformation by Cys-HB photosensitization with that of HB was made (Fig. 11(E)). The turning point (PE, in Fig. 11(E)) for HB appeared earlier than that of Cys-HB with the intensified maximum compared with Cys-HB (Fig. 11(A)), consistent with the higher $^1O_2$ generating quantum yield by HB photosensitization. It has been estimated that the rate constant of HB$^{\bullet -}$ generation was approximately 5 times as much as that for Cys-HB$^{\bullet -}$ generation [19]. So the decrease of TEMPO signal for HB was much faster than that for Cys-HB.

As is described above, the competition between active oxygen species and Cys-HB$^{\bullet -}$ generation exists in the photosensitization system and the transformation from active oxygen to Cys-HB$^{\bullet -}$ formation will take place when oxygen is exhausted. All of oxygen content, Cys-HB concentration and reaction environment affected the transformation. For different photosensitizers, the transformation and competition between Type II and Type I mechanisms are predominately controlled by the generation efficiencies of singlet oxygen and the semiquinone anion radical.

## 4. Conclusions

Active oxygen species were produced by Cys-HB photosensitization in the presence of oxygen, such as superoxide anion radical via electron transfer from Cys-HB$^{\bullet -}$ to oxygen, hydroxyl radical via the transformation from superoxide anion radical, and singlet oxygen by the energy transfer from triplet Cys-HB to oxygen. Of all, the production of singlet oxygen is predominant in the photodynamic action of Cys-HB in the presence of oxygen. The supplemental role of superoxide anion radical, hydroxyl radical and hydrogen peroxide, though, should be considered during photosensitization by Cys-HB. The depletion of oxygen in the irradiated system promoted the transformation of active oxygen species to the semiquinone anion radical of Cys-HB. Oxygen content, Cys-HB concentration and reaction environment affected this transformation process.

In terms of the production of active oxygen species, Cys-HB yielded slightly lower capacity and similar results to that of its parent hypocrellin. This indicates that cysteine-substituted hypocrellin B (Cys-HB) was photodynamic active in terms of Type II mechanism as well as Type I mechanism [19], with the significantly enhanced water-solubility and absorptivity in the range of wavelength longer than 600 nm. Investigations on the photodynamic action of Cys-HB in vivo, however, are also of great importance, and need to be undertaken.

## Acknowledgements

This research was supported by the National Natural Science Foundation of China.

## References

[1] L. J. Jiang, Chin. Sci. Bull., 21 (1990) 1608–1616 and references cited therein.
[2] Z.J. Diwu, J. Zimmermann, T. Meyer, J.W. Lown, Biochem. Pharmacol. 47 (1994) 373–385.
[3] J.B. Hudson, J. Zhou, J. Chen, L. Harris, L. Yip, G.H.N. Towers, Photochem. Photobiol. 60 (1994) 253–255.
[4] M.J. Fehr, S.L. Carpenter, Y. Wannemuehler, J.W. Petrich, Biochem. 34 (1995) 15845–15848.
[5] J. Hirayama, K. Ikebuchi, H. Abe, K.W. Kwon, Y. Ohnishi, M. Horiuch, M. Shinagawa, K. Ikuta, N. Kamo, S. Sekiquchi, Photochem. Photobiol. 66 (1997) 697–700.
[6] J.B. Hudson, V. Imperial, R.P. Haugland, Z.J. Diwu, Photochem. Photobiol. 65 (1997) 352–354.
[7] Z.J. Diwu, J.W. Lown, J. Photochem. Photobiol. A: Chem. 64 (1992) 273–287.
[8] Y.Z. Hu, J.Y. An, L.J. Jiang, J. Photochem. Phototiol. B: Biol. 17 (1993) 195–201.
[9] Y.Z. Hu, L.J. Jiang, J.Photochem. Photobiol. B: Biol. 33 (1996) 51–59.
[10] Z.J. Diwu, C.L. Zhang, J.W. Lown, Anticancer Drug Des. 8 (1993) 129–143.
[11] Z.J. Diwu, C.L. Zhang, J.W. Lown, J. Photochem. Photobiol. A: Chem. 66 (1992) 99–112.
[12] Y.Z. Hu, J.Y. An, L.J. Jiang, J. Photochem. Photobiol. B: Biol. 22 (1994) 219–227.
[13] W. Zou, J.Y. An, L.J. Jiang, Sci. Sin. (B) 26 (1996) 206–213.
[14] W. Zou, J.Y. An, L.J. Jiang, J. Photochem. Photobiol. B: Biol. 33 (1996) 73–78.
[15] Z.J. Diwu, J.W. Lown, J. Photochem. Photobiol. B: Biol. 18 (1993) 131–143.
[16] N.H. Wang, Z.Y. Zhang, J. Photochem. Photobiol. B: Biol. 14 (1992) 207–217.
[17] Z.Y. Zhang, N.H. Wang, Q. Wan, M.F. Li, Free radical Biol. Med. 14 (1993) 1–9.
[18] Y.Y. He, J.Y. An, W. Zou, L.J. Jiang, J. Photochem. Photobiol. B: Biol. 44 (1998) 45–52.
[19] Y.Y. He, J.Y. An, L.J. Jiang, J. Photochem. Photobiol. A: Chem. 115 (1998) 213–221.
[20] K.H. Zhao, L.J. Jiang, Youji Huaxue 9 (1989) 252–254.
[21] L. Ma, M.H. Zhang, L.J. Jiang, Chin. Sci. Bull. 37 (1992) 560–565 (English edition).
[22] J. Moan, E. Wold, Nature 279 (1979) 450–451.
[23] K. Lang, M. Wagnerova, P. Stopka, W. Dameran, J. Photochem. Photobiol. A: Chem. 67 (1992) 187–195.
[24] L.E. Manring, M.K. Kramer, C.S. Foote, Tetrahedron Lett. 25 (1984) 2523.
[25] C.S. Foote, Singlet Oxygen in: H.H. Wasserman, R.W. Murray (Ed.), Academic Press, New York, 1979, pp. 139–171.
[26] B.M. Monroe, J. Phys. Chem. 82 (1978) 15.
[27] T.A. Jenny, N.J. Turro, Tetrahedron 232 (1982) 2923.
[28] B.M. Monroe, J.Phys.Chem. 81 (1977) 1861–1864.
[29] A.A. Krasnovsky Jr., Chem. Phys. Lett. 18 (1981) 443.
[30] Y. Lion, E. Gandin, A. Van de Vorst, Photochem. Photobiol. 31 (1980) 305–309.